

BFLA: BLOCK-FILTERED LONG-CONTEXT ATTENTION MECHANISM

Chong Wu^{*†}
City University of Hong Kong
imroxaswc@gmail.com

Zhenan Feng[‡]
City University of Hong Kong

Renjie Xu[‡]
JD.com

Houwang Zhang[‡]
City University of Hong Kong

Jiawang Cao[‡]
Bytedance

Maolin Che^{*}
Guizhou University
chncml@outlook.com

Wenbo Zhu
University of California, Berkeley

Hong Yan
City University of Hong Kong

ABSTRACT

This paper proposes Block-Filtered Long-Context Attention (BFLA), a training-free sparse prefill attention mechanism for long-context inference. BFLA adopts a two-stage design. In Stage 1, query and key sequences are compressed into coarse blocks, and lightweight block-level softmax mass estimation is performed to construct an input-dependent block importance mask. In Stage 2, the coarse mask is expanded to the Triton attention-tile grid. Several tile-level rescue strategies are applied to reduce information loss, where a fused sparse prefill kernel skips unimportant KV tiles while preserving exact token-level attention inside every retained tile. BFLA requires no retraining, calibration, preprocessing, or model modification and can be plugged into existing vLLM-style paged-attention workloads. Experiments on Gemma 4, Llama 3.1, Qwen 3.5, and Qwen 3.6 series models show that BFLA substantially accelerates long-context prefilling with minimal accuracy degradation compared to dense Triton FlashAttention. Project website: <https://github.com/Alicewithrabbit/BFLA>.

1 INTRODUCTION

The transformer architecture (Vaswani et al., 2017) has become the dominant backbone for large language models (LLMs) (Achiam et al., 2023; Grattafiori et al., 2024). At its core lies the scaled-dot product attention (SDPA) mechanism, which captures pairwise relationships among any two tokens in a sequence. However, the quadratic computational complexity $O(N^2)$ of SDPA with respect to the sequence length N poses a major bottleneck for long-context applications. As context windows grow to 128K tokens and beyond, accelerating attention computation becomes critical for practical deployment.

Existing approaches to efficient attention can be broadly classified into three paradigms: **(1) Sparse attention**, which exploits the observation that attention matrices are approximately sparse and selectively computes only the important entries (Beltagy et al., 2020; Child et al., 2019; Xu et al., 2025; Zaheer et al., 2020; Zhang et al., 2025); **(2) Linear attention**, which replaces the softmax kernel with linear feature mapping functions to achieve $O(N)$ complexity (Choromanski et al., 2021; Han et al., 2023; Katharopoulos et al., 2020; Qin et al., 2022); and **(3) Hybrid attention**, which combines different attention mechanisms in a single unified architecture (Wu et al., 2025b; Yuan et al., 2025).

*Corresponding Author

†Project Leader

‡Equal Contribution

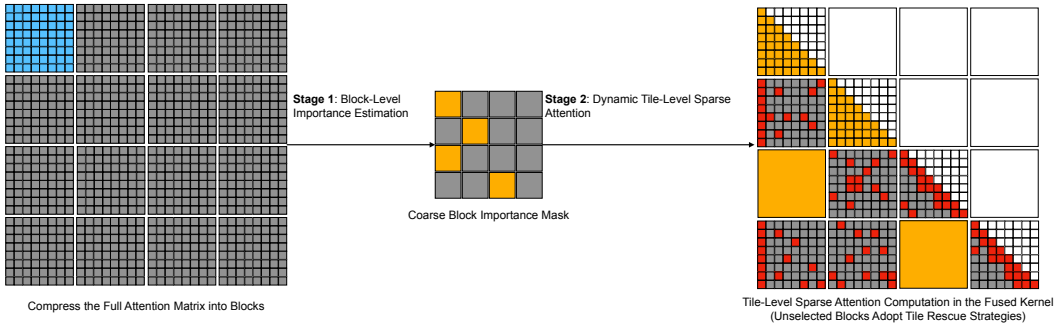


Figure 1: Overview of BFLA. **Stage 1:** Query and key sequences are compressed into coarse blocks, and block-level softmax mass estimation produces an input-dependent coarse keep mask. **Stage 2:** The coarse mask is expanded to the Triton attention-tile grid. Several tile-level rescue strategies are applied to reduce information loss, such as local band, sink, speculative rescue as shown in the figure. The fused sparse prefill kernel skips dropped KV tiles and computes exact token-level causal attention inside retained tiles. Grey regions denote skipped attention tiles.

Among these paradigms, sparse attention has a unique advantage: it preserves the original softmax attention mechanism and can directly approximate full attention output without altering the model weights. This property makes sparse attention methods particularly attractive for *plug-and-play training-free* acceleration of existing pretrained LLMs. Sparse attention methods can be further divided into two categories: **static sparse attention**, which uses fixed patterns (e.g. sliding windows (Beltagy et al., 2020; Liu et al., 2021), strided patterns (Child et al., 2019), or global tokens (Zaheer et al., 2020)) determined before runtime; and **dynamic sparse attention**, which adaptively selects important tokens or blocks based on the actual input content at inference time (Jiang et al., 2024; Tang et al., 2024; Xu et al., 2025; Zhang et al., 2025). Dynamic sparse attention has emerged as the mainstream approach because static patterns cannot capture input-dependent attention distributions.

In this paper, we propose **BFLA**, a novel dynamic dual-stage sparse attention mechanism that extends DuSA Wu et al. (2025a) for training-free prefilling acceleration of LLMs. introduces a hierarchical two-stage sparse attention strategy:

- (i) **Stage 1: block-level importance estimation.** BFLA partitions the query and KV sequences into coarse blocks, compresses each block into lightweight pooled representations, and estimates causal block importance through block-level softmax mass. The resulting mask identifies the KV blocks that should be retained for each query block and KV head.
- (ii) **Stage 2: dynamic tile-level sparse prefill attention.** The coarse block mask is expanded to the Triton attention-tile grid. A fused sparse prefill kernel skips dropped KV tiles and computes exact token-level causal attention inside every retained tile. Several tile-level rescue strategies: local band, sink, and speculative rescue can improve robustness.
- (iii) **Plug-and-play training-free acceleration.** BFLA requires no retraining, calibration, preprocessing, or weight modification. It supports runtime sparsity control and can be directly applied to existing vLLM-style paged-attention inference pipelines.

2 RELATED WORK

2.1 SPARSE ATTENTION

2.1.1 STATIC SPARSE ATTENTION

Static sparse attention methods use predetermined, input-independent patterns to reduce the number of computed attention entries. Sparse Transformer (Child et al., 2019) combines strided and local patterns to handle long sequences. Longformer (Beltagy et al., 2020) introduces a combination of sliding window attention and task-specific global tokens. BigBird (Zaheer et al., 2020) extends this with random attention connections alongside local and global patterns. Swin (Liu et al., 2021) partitions the input into non-overlapping windows and performs attention within each window. These methods achieve subquadratic complexity but rely on fixed sparsity patterns that cannot adapt to input-dependent attention distributions, often missing important long-range dependencies. CSWin (Dong et al., 2022) improves Swin by using different sparse attention in different heads. DuSA (Wu et al., 2025a) introduces a dual-stage sparse attention design to reduce global information loss.

2.1.2 DYNAMIC SPARSE ATTENTION

Dynamic sparse attention methods adaptively determine which token pairs to attend to based on the actual input content. XAttention Xu et al. (2025) uses antidiagonal scoring of the attention matrix to select important blocks for further computation. SpargeAttn Zhang et al. (2025) proposes a training-free sparse attention accelerator that predicts sparse patterns and skips unnecessary blocks during inference. MInference Jiang et al. (2024) identifies three characteristic sparse patterns (A-shape, Vertical-Slash, Block-Sparse) in long-context LLM attention heads and dynamically assigns patterns per head to accelerate refilling. Quest Tang et al. (2024) proposes query-aware KV cache page selection based on per-page key statistics, enabling efficient long-context decoding. H2O Zhang et al. (2023) introduces a heavy-hitter oracle that dynamically retains the most important tokens in the KV cache. SnapKV Li et al. (2024) identifies important KV positions using an observation window with the suffix of a prompt. StreamingLLM Xiao et al. (2024) discovers the attention sink phenomenon and combines initial tokens with a sliding window for efficient streaming inference. Our work differs from these methods by introducing a hierarchical two-stage design that combines coarse block-level importance estimation with tile-level rescue strategies and sparse execution in a fused prefill kernel, enabling training-free acceleration without modifying model weights.

2.2 LINEAR ATTENTION

Linear attention methods replace softmax operation with kernel-based feature maps to achieve linear complexity. Katharopoulos et al. (2020) reformulate attention using linear feature maps, showing that transformers can be viewed as recurrent neural networks (RNNs). Performer (Choromanski et al., 2021) uses a random feature approximation to efficiently approximate softmax attention. cosFormer Qin et al. (2022) replaces softmax with a cosine-based reweighting mechanism. FLatten (Han et al., 2023) proposes focused linear attention for vision transformers. While linear attention achieves $O(N)$ complexity, the approximation to softmax attention often introduces non-negligible accuracy degradation, especially on tasks requiring precise long-range retrieval (Yang et al., 2024). Nyströmformer (Xiong et al., 2021) and CURA (Wu et al., 2026) introduce the CUR decomposition to design linear attention, while Primal Attention (Chen et al., 2023) adopts the SVD decomposition to design linear attention. Mamba (Gu and Dao, 2023) proposes selective state space models as an alternative to attention, achieving linear-time sequence modeling.

2.3 HYBRID ATTENTION

Hybrid approaches combine multiple attention mechanisms or mix attention with other sequence modeling primitives. NSA (Yuan et al., 2025) combines compressed attention, top- k selective attention, and sliding window attention in a hardware-aligned hierarchical sparse

design. ELFATT (Wu et al., 2025b) uses parallel heads of linear attention and sparse blockify attention to capture global and local information. These methods typically require training from scratch or architectural modifications, making them less suitable for plug-and-play inference acceleration of existing LLMs.

3 METHODS

3.1 PRELIMINARIES: VANILLA SCALED-DOT PRODUCT ATTENTION

Given an input sequence of length N with embedding dimension C , the query, key, and value matrices are $\mathbf{Q}, \mathbf{K}, \mathbf{V} \in \mathbb{R}^{N \times C}$. Vanilla scaled-dot product attention (VSA) computes:

$$\mathbf{A} = \text{softmax}\left(\frac{\mathbf{Q}\mathbf{K}^\top}{\sqrt{C}}\right), \quad \mathbf{O} = \mathbf{A}\mathbf{V}, \quad (1)$$

where $\mathbf{A} \in \mathbb{R}^{N \times N}$ is the attention matrix. In multi-head attention with batch size B and H heads, the input tensors have shape (B, H, N, C) . The $O(BHN^2C)$ complexity of VSA dominates the computational cost of the prefilling stage in LLMs. For clarity, all vectors appearing in this paper are assumed to be row vectors.

3.2 STAGE 1: BLOCK-LEVEL IMPORTANCE ESTIMATION

Notation. Let the query tensor and key tensor be written in head-first layout:

$$\mathcal{Q} \in \mathbb{R}^{H_q \times N_q \times C}, \quad \mathcal{K} \in \mathbb{R}^{H_{kv} \times N_{kv} \times C}, \quad (2)$$

where N_q is the number of query tokens in the current prefill or chunked-prefill request, N_{kv} is the number of tokens in the full KV sequence, H_q is the number of query heads, H_{kv} is the number of KV heads, and C is the per-head channel dimension.

For grouped-query attention (GQA), we have

$$H_q = mH_{kv}, \quad m = \frac{H_q}{H_{kv}},$$

where m is the number of query heads associated with each KV head.

Let b be the coarse block size used by BFLA. The number of query blocks and KV blocks are

$$L_q = \left\lceil \frac{N_q}{b} \right\rceil, \quad L_{kv} = \left\lceil \frac{N_{kv}}{b} \right\rceil.$$

After padding and block partitioning, we obtain

$$\mathcal{Q}_{\text{block}} \in \mathbb{R}^{H_q \times L_q \times b \times C}, \quad \mathcal{K}_{\text{block}} \in \mathbb{R}^{H_{kv} \times L_{kv} \times b \times C}.$$

Flattening- g block pooling. For flattening- g block pooling, let

$$G = \frac{b}{g}.$$

Each block is divided into G token groups, and each group is flattened into a vector of dimension gC . Therefore,

$$\Phi(\mathcal{Q}) \in \mathbb{R}^{H_q \times L_q \times G \times gC}, \quad \Phi(\mathcal{K}) \in \mathbb{R}^{H_{kv} \times L_{kv} \times G \times gC}.$$

GQA head grouping. For the h -th KV head, the associated query head group is

$$\mathbb{H}_h = \{hm, hm + 1, \dots, hm + m - 1\}, \quad h \in \{0, \dots, H_{kv} - 1\}.$$

Block-level importance estimation. For each query head $p \in \mathbb{H}_h$, query block i , KV block j , query group u , and KV group v , the group-level score is

$$\mathcal{S}_{h,p,i,j,u,v} = \Phi(\mathcal{Q})_{p,i,u} \Phi(\mathcal{K})_{h,j,v}^\top, \quad (3)$$

where

$$i \in \{0, \dots, L_q - 1\}, \quad j \in \{0, \dots, L_{kv} - 1\}, \quad u, v \in \{0, \dots, G - 1\}.$$

The block-level importance score is obtained by max-pooling over all group pairs:

$$\mathcal{S}_{h,p,i,j} = \max_{u,v} \mathcal{S}_{h,p,i,j,u,v}. \quad (4)$$

Causal masking. Let $N_c = N_{kv} - N_q$ be the context length before the current query chunk. The absolute end position of query block i is

$$e_i = \min(N_c + (i + 1)b - 1, N_{kv} - 1), \quad (5)$$

and the start position of KV block j is

$$p_j = jb. \quad (6)$$

The causal block mask is

$$\mathcal{M}_{i,j}^{\text{causal}} = \mathbf{1}[p_j \leq e_i]. \quad (7)$$

Non-causal scores are masked as

$$\mathcal{S}_{h,p,i,j} = -\infty, \quad \text{if } \mathcal{M}_{i,j}^{\text{causal}} = 0. \quad (8)$$

Block-level full attention. For each query head p , query block i , and KV head h , the normalized block probability is

$$\mathcal{A}_{h,p,i,j} = \frac{\exp(\alpha \mathcal{S}_{h,p,i,j})}{\sum_{j'=0}^{L_{kv}-1} \exp(\alpha \mathcal{S}_{h,p,i,j'})}, \quad (9)$$

where

$$\alpha = \frac{1}{\sqrt{C}}.$$

Keep-mass selection. For each (h, p, i) , sort the KV blocks by descending probability:

$$\mathcal{A}_{h,p,i,\pi_1} \geq \mathcal{A}_{h,p,i,\pi_2} \geq \dots \geq \mathcal{A}_{h,p,i,\pi_{L_{kv}}}. \quad (10)$$

Given the mass threshold $\gamma \leq 1$, choose the smallest r^* such that

$$\sum_{t=1}^{r^*} \mathcal{A}_{h,p,i,\pi_t} \geq \gamma. \quad (11)$$

The mass-based keep mask for query head p is

$$\mathcal{M}_{h,p,i,j}^{\text{mass}} = \mathbf{1}[j \in \{\pi_1, \dots, \pi_{r^*}\}]. \quad (12)$$

Expansion to the Triton tile mask. The sparse attention kernel operates on the Triton attention tile grid with tile size T . When b is an integer multiple of T , define

$$\rho_b = \frac{b}{T}. \quad (13)$$

For current request r , the coarse block mask is expanded to the tile-level execution mask by

$$\mathcal{M}_{r,h,i\rho_b+u,j\rho_b+v}^{\text{tile}} = \mathcal{M}_{r,h,i,j}^{\text{mass}}, \quad u, v \in \{0, \dots, \rho_b - 1\}. \quad (14)$$

3.3 STAGE 2: DYNAMIC TILE-LEVEL SPARSE ATTENTION

Tile-level local band sink rescue. Let T denote the Triton attention tile size. For current query tile i and KV tile j , the actual local window size at the tile-level is

$$\mathcal{M}_{r,h,i,j-v}^{\text{tile}} = \mathbf{1} \quad (15)$$

where

$$\max(0, j - n_{\text{local}}) \leq v \leq j.$$

The attention sink is also preserved at the tile level:

$$\mathcal{M}_{r,h,i,j}^{\text{tile}} = \mathbf{1}[j < T]. \quad (16)$$

Tile-level speculative rescue. After mass selection, local band rescue, and sink rescue, the dropped causal blocks are

$$\mathcal{D}_{r,h,i,j} = \mathbf{1} \wedge \neg \mathcal{M}_{r,h,i,j}^{\text{tile}}. \quad (17)$$

For stride-based rescue, with a stride size of η and seed s , BFLA deterministically rescues a subset of dropped tiles:

$$\mathcal{D}_{r,h,i,j}^{\text{stride}} = \mathbf{0} [\chi(i, j; s) \bmod \eta = 0], \quad (18)$$

where $\chi(i, j; s)$ is a lightweight deterministic mixing function.

For random rescue, with probability $\rho \leq 1$, BFLA rescues tiles dropped according to a pseudo-random deterministic mapping:

$$\mathcal{D}_{r,h,i,j}^{\text{rand}} = \mathbf{0} [\psi(h, i, j; s) < \rho], \quad \psi(h, i, j; s) \in [0, 1), \quad (19)$$

where ψ is parameterized by seed s .

Final coarse BFLA mask. The final coarse block mask is

$$\mathcal{M}_{r,h,i,j}^{\text{tile}} = \mathcal{M}_{r,h,i,j}^{\text{tile}} \vee (\neg \mathcal{D}_{r,h,i,j}^{\text{spec}}) \vee (\neg \mathcal{D}_{r,h,i,j}^{\text{rand}}). \quad (20)$$

An example of $\mathcal{M}^{\text{tile}}$ is shown in Fig. 1. The large orange blocks denote the coarse blocks selected by mass estimation. The small red tiles are selected by tile-level rescue strategies.

Final sparse attention. For each request r , query head p , and its associated KV head h , BFLA computes the exact attention over the selected KV tiles:

$$\mathcal{A}_{r,p,i,j} = \text{softmax} \left(\frac{\mathcal{Q}_{r,p,i} \mathcal{K}_{r,h,j}^\top + \mathfrak{M}_{r,h,i,j}}{\sqrt{C}} \right), \quad \mathcal{O}_{r,p,i} = \mathcal{A}_{r,p,i,j} \mathcal{V}_{r,h,j}. \quad (21)$$

Here, $\mathfrak{M}_{r,h,i,j}$ is the additive dynamic tile-level mask induced by $\mathcal{M}_{r,h,i,j}^{\text{tile}}$. The entries belonging to the dropped tiles are filled with $-\infty$, while the remaining tiles still use exact token-level causal masking inside the fused attention kernel. Therefore, BFLA skips selected KV tiles, but the attention computation inside each kept tile remains exact. This avoids materializing the sparse attention matrix and reduces memory I/O.

Complexity analysis. Let κ denote the final fraction of causal KV tiles kept by the tile-level mask $\mathcal{M}^{\text{tile}}$, after block selection and tile rescue. For full attention, the prefill complexity is

$$O(H_q N_q N_{kv} C). \quad (22)$$

In Stage 2, BFLA computes attention only over the kept KV tiles. Therefore, the sparse prefill attention complexity becomes

$$O(\kappa H_q N_q N_{kv} C). \quad (23)$$

For Stage 1, BFLA builds the sparse mask using lightweight block-level scores. With flattening- g pooling, each coarse block is divided into $G = b/g$ groups, and each group is flattened into a vector of dimension gC . The block-score estimation cost is

$$O(H_q L_q L_{kv} G^2 gC) = O \left(H_q \frac{N_q}{b} \frac{N_{kv}}{b} \left(\frac{b}{g} \right)^2 gC \right) = O \left(H_q \frac{N_q N_{kv} C}{g} \right). \quad (24)$$

The keep-mass sorting introduces an additional lower-order term

$$O(H_q L_q L_{kv} \log L_{kv}), \quad (25)$$

which is typically small compared with token-level attention computation.

Thus, the total BFLA prefill complexity is approximately

$$O\left(H_q \frac{N_q N_{kv} C}{g} + \kappa H_q N_q N_{kv} C\right). \quad (26)$$

For non-chunked prefill where $N_q = N_{kv} = N$, this becomes

$$O\left(H_q \frac{N^2 C}{g} + \kappa H_q N^2 C\right). \quad (27)$$

When g (BFLA adopts $g = 64$ for most cases) is large and $\kappa \ll 1$, BFLA significantly reduces the dominant prefill attention cost while preserving exact token-level attention inside every kept tile. The upper bounds analysis for dual stage sparse attention design is available in Section 6.

4 EXPERIMENTS AND RESULTS

4.1 EXPERIMENTAL SETUP

We evaluate BFLA along two axes: inference efficiency and task fidelity. The efficiency evaluation focuses on the prefilling stage, where the computational cost of full attention becomes increasingly dominant as the context length grows. Quality evaluation examines whether BFLA can replace full attention without degrading reasoning, coding, knowledge, and long-context capabilities of pretrained large language models.

We conduct experiments on several representative instruction-tuned models, including Gemma 4-E4B DeepMind (2026), Gemma 4-31B DeepMind (2026), Llama 3.1-8B Grattafiori et al. (2024), Qwen 3.5-9B Team (2026a), and Qwen 3.6-27B Team (2026b). For each model, we replace all full-attention layers with BFLA while keeping the original model weights unchanged. No fine-tuning, calibration, or additional preprocessing is applied. This setting directly evaluates BFLA as a replacement for drop-in sparse attention for existing foundation models.

We evaluate the quality of the model on AIME 2026 Dekoninck et al. (2026), GPQA Diamond Rein et al. (2024), LiveCodeBench v6 Jain et al. (2025), LongBench Bai et al. (2024), and MMLU Pro Wang et al. (2024). These benchmarks cover mathematical reasoning, scientific question answering, code generation, long-context understanding, and broad professional knowledge. All speed and benchmark experiments are conducted on 8 NVIDIA A100 80GB GPUs.

Baselines. We compare BFLA with the following attention implementations:

- **TFA**: the dense full-attention baseline implemented with the Triton FlashAttention kernel in vLLM (0.19.1).
- **XAttention** Xu et al. (2025): a block-sparse attention method that selects important blocks using antidiagonal scoring.

4.2 PREFILLING EFFICIENCY

Tables 1 and 2 report the prefilling latency and throughput of full attention (TFA) and BFLA on Gemma 4-E4B and Qwen 3.6-27B. The results show a clear context-length-dependent acceleration pattern. At 2K tokens, BFLA is slightly slower than full attention, achieving $0.952\times$ speedup on Gemma 4-E4B and $0.969\times$ speedup on Qwen 3.6-27B. This is expected because, at short sequence lengths, the overhead of sparse mask building and block selection cannot yet be covered by the reduced attention computation.

Table 1: Prefilling efficiency comparison between TFA and BFLA on Gemma 4-E4B across different context lengths. Speedup is computed relative to TFA.

Context Len	TFA (s)	TFA Throughput (tok/s)	BFLA (s)	BFLA Throughput (tok/s)	Speedup
2K	0.0551	37172	0.0579	35384	0.952x / -4.8%
4K	0.0945	43349	0.0913	44849	1.035x / +3.5%
8K	0.1690	48466	0.1563	52408	1.081x / +8.1%
16K	0.3651	44872	0.3130	52352	1.166x / +16.6%
32K	0.7868	41646	0.5919	55365	1.329x / +32.9%
64K	1.9658	33337	1.1871	55208	1.656x / +65.6%
128K	5.6839	23060	2.4993	52444	2.274x / +127.4%

Table 2: Prefilling efficiency comparison between TFA and BFLA on Qwen 3.6-27B across different context lengths. Speedup is computed relative to TFA.

Context Len	TFA (s)	TFA TPS (tok/s)	BFLA Time (s)	BFLA TPS (tok/s)	Speedup
2K	0.1487	13776	0.1534	13355	0.969x / -3.1%
4K	0.2500	16385	0.2390	17140	1.046x / +4.6%
8K	0.4523	18113	0.4217	19427	1.073x / +7.3%
16K	0.9698	16895	0.8133	20145	1.192x / +19.2%
32K	2.3092	14190	1.6744	19570	1.379x / +37.9%
64K	6.0680	10800	3.3925	19318	1.789x / +78.9%
128K	18.1649	7216	7.2644	18043	2.501x / +150.1%

When the context length increases, BFLA consistently outperforms full attention. On Gemma 4-E4B, the speedup increases from 1.035 \times at 4K to 1.329 \times at 32K, and further reaches 2.274 \times at 128K. At 128K tokens, the prefilling throughput improves from 23,060 tokens/s under full attention to 52,444 tokens/s under BFLA. The same trend is observed on the larger Qwen 3.6-27B model, where BFLA reduces the 128K prefilling time from 18.1649s to 7.2644s and improves the throughput from 7,216 tokens/s to 18,043 tokens/s, corresponding to a 2.501 \times speedup.

These results demonstrate that BFLA is particularly effective in the long-context regime. Although many modern LLMs adopt hybrid architectures and use full attention only in a subset of layers, replacing these full attention layers is still sufficient to produce substantial prefilling acceleration. This confirms the practical value of BFLA for long-context inference, where prefilling efficiency is often a major deployment bottleneck.

4.3 LONG-CONTEXT UNDERSTANDING

Table 3 compares TFA, BFLA, and XAttention on LongBench. Full attention achieves an average score of 0.4022, while BFLA obtains 0.3975 and XAttention obtains 0.3976. The average gap between BFLA and full attention is only 0.0047, indicating that BFLA preserves most of the long-context understanding capability while using a sparse attention pattern.

At the task level, BFLA performs competitively across diverse long-context scenarios. It improves over full attention on several tasks, including LCC, MultiNews, MultiFieldQA-en, MultiFieldQA-zh, QMSum, RepoBench-P, TriviaQA, and VCSum. For example, BFLA improves MultiFieldQA-en from 0.4050 to 0.4177 and RepoBench-P from 0.3231 to 0.3311. These gains suggest that the sparse pattern selected by BFLA can preserve important long-range dependencies for some comprehension and summarization tasks.

BFLA shows modest degradation on some retrieval-heavy or counting-oriented tasks, such as PassageCount and PassageRetrieval. This suggests that tasks requiring very fine-grained token-level evidence may be more sensitive to aggressive sparsification. Nevertheless, BFLA remains close to XAttention in average LongBench score, showing that it can match a strong sparse-attention baseline in long-context quality while offering advantages in mask construction efficiency, as analyzed later.

4.4 GENERAL BENCHMARK PERFORMANCE

Table 4 compares full attention (TFA) and BFLA across multiple models and general-purpose benchmarks. The results show that BFLA preserves the core capabilities of the original

Table 3: Comparison of full attention, BFLA, and XAttention on LongBench.

Task	Full	BFLA	XAttention
2WikiMQA	0.2471	0.2365	0.2504
Dureader	0.2967	0.2963	0.2959
GovReport	0.3490	0.3438	0.3469
HotpotQA	0.3272	0.3153	0.3238
LCC	0.3333	0.3335	0.3364
LSHT	0.4600	0.4550	0.4300
MultiNews	0.2696	0.2698	0.2687
MultiFieldQA-en	0.4050	0.4177	0.4048
MultiFieldQA-zh	0.2016	0.2022	0.2022
MuSiQue	0.1757	0.1717	0.1713
NarrativeQA	0.3137	0.3025	0.2984
PassageCount	0.0883	0.0663	0.0700
PassageRetrieval-en	0.9534	0.9272	0.9193
PassageRetrieval-zh	0.9293	0.9131	0.9218
Qasper	0.2840	0.2776	0.2789
QMSum	0.2350	0.2385	0.2330
RepoBench-P	0.3231	0.3311	0.3271
SAMSum	0.4390	0.4371	0.4387
TREC	0.7300	0.7250	0.7450
TriviaQA	0.9213	0.9216	0.9203
VCSum	0.1642	0.1651	0.1670
Average	0.4022	0.3975	0.3976

Table 4: Performance comparison between full attention and BFLA across models and benchmarks. Higher scores indicate better performance. Reported scores may differ from official reports due to differences in seeds, kernels, precision, hardware, and evaluation settings. For fairness, all comparisons in this table use the same seeds, hardware, kernel implementation, precision, and evaluation protocol; the only changed component is the attention mechanism.

Benchmarks	Qwen 3.5-9B	Qwen 3.5-9B-BFLA	Qwen 3.6-27B	Qwen 3.6-27B-BFLA	Gemma 4-E4B	Gemma 4-E4B-BFLA	Gemma 4-31B	Gemma 4-31B-BFLA
MMLU Pro (EM)	81.4%	81.4%	83.3%	83.2%	68.4%	68.8%	84.9%	84.9%
AIME 2026 no tools (EM)	90.0%	90.0%	93.3%	93.3%	43.3%	43.3%	86.7%	86.7%
GPQA Diamond (EM)	83.3%	82.3%	84.3%	84.3%	53.5%	54.6%	79.8%	81.8%
LiveCodeBench v6 (Pass@1)	64.7%	65.5%	77.3%	77.3%	62.0%	62.0%	77.7%	77.7%

pretrained models. Across the evaluated model–benchmark pairs, BFLA closely matches full attention, with small variations in both directions under the same evaluation protocol.

On MMLU Pro, BFLA produces nearly identical results to full attention. Qwen 3.5-9B remains at 81.4%, Qwen 3.6-27B changes only slightly from 83.3% to 83.2%, Gemma 4-E4B improves from 68.4% to 68.8%, and Gemma 4-31B remains at 84.9%. On AIME 2026, BFLA exactly matches full attention for all evaluated models, including 90.0% on Qwen 3.5-9B, 93.3% on Qwen 3.6-27B, 43.3% on Gemma 4-E4B, and 86.7% on Gemma 4-31B.

The results on GPQA Diamond and LiveCodeBench v6 further support the stability of BFLA. On GPQA Diamond, BFLA slightly decreases Qwen 3.5-9B from 83.3% to 82.3%, keeps Qwen 3.6-27B unchanged at 84.3%, improves Gemma 4-E4B from 53.5% to 54.6%, and improves Gemma 4-31B from 79.8% to 81.8%. On LiveCodeBench v6, BFLA matches full attention on Qwen 3.6-27B, Gemma 4-E4B, and Gemma 4-31B, while improving Qwen 3.5-9B from 64.7% to 65.5%.

In general, these results indicate that BFLA accelerates the prefilling stage without introducing systematic accuracy degradation. Since all model weights, seeds, hardware, precision settings, and evaluation protocols are kept fixed, the only changed component is the attention mechanism. Therefore, the observed performance stability suggests that BFLA is a faithful sparse approximation to full attention for pretrained foundation models.

Table 5: Overall mask tile-level density/sparsity and mask construction overhead on LongBench using Llama 3.1-8B.

Method	Avg. Score	Density	Sparsity	Avg. Mask Build
BFLA $b = 256, g = 64, \gamma = 0.95, n_{\text{local}} = 8, \rho = 0, \text{no } \eta$	38.21	8.75%	91.25%	1.65 ms
BFLA $b = 256, g = 64, \gamma = 0.999, n_{\text{local}} = 8, \rho = 0, \text{no } \eta$	38.79	8.85%	91.15%	1.70 ms
BFLA $b = 256, g = 64, \gamma = 0.95, n_{\text{local}} = 8, \rho = 0, \eta = 16$	38.36	14.40%	85.60%	1.78 ms
BFLA $b = 256, g = 64, \gamma = 0.95, n_{\text{local}} = 16, \rho = 0, \eta = 16$	38.87	16.87%	83.13%	1.88 ms
BFLA $b = 256, g = 64, \gamma = 0.98, n_{\text{local}} = 8, \rho = 0, \eta = 16$	38.87	14.62%	85.38%	1.94 ms
BFLA $b = 256, g = 64, \gamma = 0.99, n_{\text{local}} = 8, \rho = 0, \eta = 16$	39.40	14.65%	85.35%	1.76 ms
BFLA $b = 128, g = 64, \gamma = 0.99, n_{\text{local}} = 8, \rho = 0.1, \eta = 16$	39.36	20.62%	79.38%	2.10 ms
BFLA $b = 256, g = 64, \gamma = 0.99, n_{\text{local}} = 8, \rho = 0.1, \eta = 16$	39.75	29.57%	70.43%	2.08 ms
BFLA $b = 256, g = 256, \gamma = 0.99, n_{\text{local}} = 8, \rho = 0.1, \eta = 16$	38.26	19.85%	80.15%	1.72 ms
BFLA $b = 512, g = 64, \gamma = 0.99, n_{\text{local}} = 8, \rho = 0.1, \eta = 16$	39.81	28.00%	72.00%	2.27 ms
BFLA $b = 512, g = 128, \gamma = 0.99, n_{\text{local}} = 8, \rho = 0.1, \eta = 16$	39.76	27.32%	72.68%	2.06 ms
BFLA $b = 1024, g = 64, \gamma = 0.99, n_{\text{local}} = 8, \rho = 0.1, \eta = 16$	40.00	43.37%	56.63%	2.06 ms
XAttention	39.76	13.41%	86.59%	7.82 ms
Dense	40.22	-	-	-

4.5 SPARSITY AND MASK-CONSTRUCTION ANALYSIS

Table 5 reports the average LongBench score, mask density, sparsity, and mask-construction overhead of different BFLA configurations on Llama 3.1-8B. We also compare BFLA with XAttention and full attention. This experiment evaluates whether BFLA can provide a favorable balance between sparsity, accuracy, and runtime overhead.

The results show that BFLA supports a wide range of accuracy–sparsity trade-offs. Highly sparse configurations can retain less than 10% of attention tiles. For example, the configuration with $b = 256, g = 64, \gamma = 0.95, n_{\text{local}} = 8, \rho = 0$ and no η keeps only 8.75% of KV tiles, corresponding to 91.25% sparsity, while achieving a LongBench score of 38.21 with only 1.65 ms mask-construction overhead. Increasing the retained mass or enabling the rescue parameter η improves the LongBench score while keeping the mask-building cost low.

A strong operating point is achieved by $b = 256, g = 64, \gamma = 0.99, n_{\text{local}} = 8, \rho = 0, \eta = 16$. This configuration obtains a LongBench score of 39.40 with 14.65% density, 85.35% sparsity, and 1.76 ms average mask-construction overhead. Compared with XAttention, which obtains a similar score of 39.76 with 13.41% density but requires 7.82ms for mask construction, this BFLA configuration reduces mask-building overhead by nearly 5 \times .

When more attention tiles are retained, BFLA can further approach dense-attention quality. For example, the configuration with $b = 1024, g = 64, \gamma = 0.99, n_{\text{local}} = 8, \rho = 0.1, \eta = 16$ achieves a score of 40.00, close to the dense-attention score of 40.22, while still maintaining 56.63% sparsity and only 2.06 ms mask-construction overhead. This shows that BFLA can flexibly trade sparsity for quality depending on deployment requirements.

Overall, the sparsity results demonstrate that BFLA is not only accurate but also system-friendly. It achieves competitive LongBench performance with high sparsity and substantially lower mask-construction overhead than XAttention. This property is important for practical inference systems, where the overhead of constructing sparse masks can otherwise offset the computational benefit of sparse attention.

5 CONCLUSIONS

In this paper, we propose BFLA, a training-free sparse prefill attention mechanism for long-context LLM inference. BFLA first estimates block-level importance using lightweight pooled query and key representations, then expands the resulting coarse mask to the Triton tile grid for fused sparse prefill execution. The kernel skips unimportant KV tiles while preserving exact token-level causal attention inside every retained tile. Using several tile-level rescue strategies, the robustness is improved without sacrificing too much speed. Across Gemma 4, Llama 3.1, Qwen 3.5, and Qwen 3.6 series models, BFLA provides substantial long-context prefill speedups with minimal accuracy degradation on reasoning, coding, knowledge, and long-context benchmarks. These results demonstrate that BFLA is a practical plug-and-play sparse attention backend for vLLM-style inference systems.

REFERENCES

- Josh Achiam, Steven Adler, Sandhini Agarwal, Lama Ahmad, Ilge Akkaya, Florencia Leoni Aleman, Diogo Almeida, Janko Altenschmidt, Sam Altman, Shyamal Anadkat, et al. GPT-4 technical report. *arXiv preprint arXiv:2303.08774*, 2023.
- Yushi Bai, Xin Lv, Jiajie Zhang, Hongchang Lyu, Jiankai Tang, Zhidian Huang, Zhengxiao Du, Xiao Liu, Aohan Zeng, Lei Hou, Yuxiao Dong, Jie Tang, and Juanzi Li. LongBench: A bilingual, multitask benchmark for long context understanding. In Lun-Wei Ku, Andre Martins, and Vivek Srikumar, editors, *Proceedings of the 62nd Annual Meeting of the Association for Computational Linguistics (Volume 1: Long Papers)*, pages 3119–3137. Association for Computational Linguistics, 2024. doi: 10.18653/v1/2024.acl-long.172. URL <https://aclanthology.org/2024.acl-long.172/>.
- Iz Beltagy, Matthew E. Peters, and Arman Cohan. Longformer: The long-document transformer. *CoRR*, abs/2004.05150, 2020. URL <https://arxiv.org/abs/2004.05150>.
- Yingyi Chen, Qinghua Tao, Francesco Tonin, and Johan Suykens. Primal-Attention: Self-attention through asymmetric kernel SVD in primal representation. In A. Oh, T. Naumann, A. Globerson, K. Saenko, M. Hardt, and S. Levine, editors, *Advances in Neural Information Processing Systems*, volume 36, pages 65088–65101. Curran Associates, Inc., 2023.
- Rewon Child, Scott Gray, Alec Radford, and Ilya Sutskever. Generating long sequences with sparse transformers. *CoRR*, abs/1904.10509, 2019. URL <https://arxiv.org/abs/1904.10509>.
- Krzysztof Marcin Choromanski, Valerii Likhoshesterov, David Dohan, Xingyou Song, Andreea Gane, Tamas Sarlos, Peter Hawkins, Jared Quincy Davis, Afroz Mohiuddin, Łukasz Kaiser, David Benjamin Belanger, Lucy J Colwell, and Adrian Weller. Rethinking attention with performers. In *International Conference on Learning Representations*, 2021. URL <https://openreview.net/forum?id=Ua6zuk0WRH>.
- Google DeepMind. Gemma 4: Frontier multimodal intelligence on device, April 2026. URL <https://blog.google/innovation-and-ai/technology/developers-tools/gemma-4>.
- Jasper Dekoninck, Nikola Jovanović, Tim Gehringer, Kári Rognvaldsson, Ivo Petrov, Chenhao Sun, and Martin Vechev. Beyond benchmarks: MathArena as an evaluation platform for mathematics with LLMs. 2026. URL <https://arxiv.org/abs/2605.00674>.
- Xiaoyi Dong, Jianmin Bao, Dongdong Chen, Weiming Zhang, Nenghai Yu, Lu Yuan, Dong Chen, and Baining Guo. CSWin transformer: A general vision transformer backbone with cross-shaped windows. In *Proceedings of the IEEE/CVF Conference on Computer Vision and Pattern Recognition (CVPR)*, pages 12124–12134, 2022.
- Aaron Grattafiori, Abhimanyu Dubey, Abhinav Jauhri, Abhinav Pandey, Abhishek Kadian, Ahmad Al-Dahle, Aiesha Letman, Akhil Mathur, Alan Schelten, Alex Vaughan, et al. The Llama 3 herd of models. *arXiv preprint arXiv:2407.21783*, 2024.
- Albert Gu and Tri Dao. Mamba: Linear-time sequence modeling with selective state spaces. *arXiv preprint arXiv:2312.00752*, 2023.
- Dongchen Han, Xuran Pan, Yizeng Han, Shiji Song, and Gao Huang. FLatten transformer: Vision transformer using focused linear attention. In *Proceedings of the IEEE/CVF International Conference on Computer Vision (ICCV)*, pages 5961–5971, 2023.
- Naman Jain, King Han, Alex Gu, Wen-Ding Li, Fanjia Yan, Tianjun Zhang, Sida Wang, Armando Solar-Lezama, Koushik Sen, and Ion Stoica. Livecodebench: Holistic and contamination free evaluation of large language models for code. In *The Thirteenth International Conference on Learning Representations*, 2025. URL <https://openreview.net/forum?id=chfJJYC3iL>.

- Huiqiang Jiang, Yucheng Li, Chengruidong Zhang, Qianhui Wu, Xufang Luo, Surin Ahn, Zhenhua Han, Amir H Abdi, Dongsheng Li, Chin-Yew Lin, Yuqing Yang, and Lili Qiu. MInference 1.0: Accelerating pre-filling for long-context LLMs via dynamic sparse attention. In *Advances in Neural Information Processing Systems*, volume 37, 2024.
- Angelos Katharopoulos, Apoorv Vyas, Nikolaos Pappas, and François Fleuret. Transformers are RNNs: Fast autoregressive transformers with linear attention. In Hal Daumé III and Aarti Singh, editors, *Proceedings of the 37th International Conference on Machine Learning*, volume 119 of *Proceedings of Machine Learning Research*, pages 5156–5165. PMLR, 2020. URL <https://proceedings.mlr.press/v119/katharopoulos20a.html>.
- Yuhong Li, Yingbing Huang, Bowen Yang, Bharat Venkitesh, Acyr Locatelli, Hanchen Ye, Tianle Cai, Patrick Lewis, and Deming Chen. SnapKV: LLM knows what you are looking for before generation. *arXiv preprint arXiv:2404.14469*, 2024.
- Ze Liu, Yutong Lin, Yue Cao, Han Hu, Yixuan Wei, Zheng Zhang, Stephen Lin, and Baining Guo. Swin transformer: Hierarchical vision transformer using shifted windows. In *Proceedings of the IEEE/CVF International Conference on Computer Vision (ICCV)*, pages 10012–10022, 2021.
- Zhen Qin, Weixuan Sun, Hui Deng, Dongxu Li, Yunshen Wei, Baohong Lv, Junjie Yan, Lingpeng Kong, and Yiran Zhong. cosFormer: Rethinking softmax in attention. In *International Conference on Learning Representations*, 2022. URL <https://openreview.net/forum?id=B18CQrx2Up4>.
- David Rein, Betty Li Hou, Asa Cooper Stickland, Jackson Petty, Richard Yuanzhe Pang, Julien Dirani, Julian Michael, and Samuel R. Bowman. GPQA: A graduate-level google-proof Q&A benchmark. In *First Conference on Language Modeling*, 2024. URL <https://openreview.net/forum?id=Ti67584b98>.
- Jiaming Tang, Yilong Zhao, Kan Zhu, Guangxuan Xiao, Baris Kasikci, and Song Han. Quest: Query-aware sparsity for efficient long-context LLM inference. In *Proceedings of the 41st International Conference on Machine Learning*. PMLR, 2024.
- Qwen Team. Qwen3.5: Accelerating productivity with native multimodal agents, February 2026a. URL <https://qwen.ai/blog?id=qwen3.5>.
- Qwen Team. Qwen3.6-27b: Flagship-level coding in a 27b dense model, April 2026b. URL <https://qwen.ai/blog?id=qwen3.6-27b>.
- Ashish Vaswani, Noam Shazeer, Niki Parmar, Jakob Uszkoreit, Llion Jones, Aidan N Gomez, Łukasz Kaiser, and Illia Polosukhin. Attention is all you need. In I. Guyon, U. Von Luxburg, S. Bengio, H. Wallach, R. Fergus, S. Vishwanathan, and R. Garnett, editors, *Advances in Neural Information Processing Systems*, volume 30, pages 5998–6008. Curran Associates, Inc., 2017.
- Yubo Wang, Xueguang Ma, Ge Zhang, Yuansheng Ni, Abhranil Chandra, Shiguang Guo, Weiming Ren, Aaran Arulraj, Xuan He, Ziyang Jiang, Tianle Li, Max Ku, Kai Wang, Alex Zhuang, Rongqi Fan, Xiang Yue, and Wenhui Chen. MMLU-Pro: A more robust and challenging multi-task language understanding benchmark. In A. Globerson, L. Mackey, D. Belgrave, A. Fan, U. Paquet, J. Tomczak, and C. Zhang, editors, *Advances in Neural Information Processing Systems*, volume 37, pages 95266–95290. Curran Associates, Inc., 2024. doi: 10.52202/079017-3018.
- Chong Wu, Jiawang Cao, Renjie Xu, Zhuoheng Ran, Maolin Che, Wenbo Zhu, and Hong Yan. Dusa: Fast and accurate dual-stage sparse attention mechanism accelerating both training and inference. In D. Belgrave, C. Zhang, H. Lin, L. Montoya, R. Pascanu, P. Koniusz, M. Ghassemi, and N. Chen, editors, *Advances in Neural Information Processing Systems*, volume 38, pages 41087–41113. Curran Associates, Inc., 2025a.
- Chong Wu, Maolin Che, Renjie Xu, Zhuoheng Ran, and Hong Yan. ELFATT: Efficient linear fast attention for vision transformers. In *Proceedings of the 33rd ACM International*

- Conference on Multimedia*, MM '25, pages 9140–9149, New York, NY, USA, 2025b. Association for Computing Machinery. doi: 10.1145/3746027.3754825. URL <https://doi.org/10.1145/3746027.3754825>.
- Chong Wu, Maolin Che, and Hong Yan. The CUR decomposition of self-attention matrices in vision transformers. *IEEE Transactions on Pattern Analysis and Machine Intelligence*, 48(4):4792–4809, 2026. doi: 10.1109/TPAMI.2025.3646452.
- Guangxuan Xiao, Yuandong Tian, Beidi Chen, Song Han, and Mike Lewis. Efficient streaming language models with attention sinks. In *International Conference on Learning Representations*, 2024. URL <https://openreview.net/forum?id=NG7sS51zVF>.
- Yunyang Xiong, Zhanpeng Zeng, Rudrasis Chakraborty, Mingxing Tan, Glenn Fung, Yin Li, and Vikas Singh. Nyströmformer: A Nyström-based algorithm for approximating self-attention. In *Proceedings of the AAAI Conference on Artificial Intelligence*, volume 35, pages 14138–14148, 2021. doi: 10.1609/aaai.v35i16.17664.
- Ruyi Xu, Guangxuan Xiao, Haofeng Huang, Junxian Guo, and Song Han. XAttention: Block sparse attention with antidiagonal scoring. In Aarti Singh, Maryam Fazel, Daniel Hsu, Simon Lacoste-Julien, Felix Berkenkamp, Tegan Maharaj, Kiri Wagstaff, and Jerry Zhu, editors, *Proceedings of the 42nd International Conference on Machine Learning*, volume 267 of *Proceedings of Machine Learning Research*, pages 69819–69831. PMLR, 2025. URL <https://proceedings.mlr.press/v267/xu25ag.html>.
- Kai Yang, Jan Ackermann, Zhenyu He, Guhao Feng, Bohang Zhang, Yunzhen Feng, Qiwei Ye, Di He, and Liwei Wang. Do efficient transformers really save computation?, 2024. URL <https://arxiv.org/abs/2402.13934>.
- Jingyang Yuan, Huazuo Gao, Damai Dai, Junyu Luo, Liang Zhao, Zhengyan Zhang, Zhenda Xie, Yuxing Wei, Lean Wang, Zhiping Xiao, Yuqing Wang, Chong Ruan, Ming Zhang, Wenfeng Liang, and Wangding Zeng. Native sparse attention: Hardware-aligned and natively trainable sparse attention. In Wanxiang Che, Joyce Nabende, Ekaterina Shutova, and Mohammad Taher Pilehvar, editors, *Proceedings of the 63rd Annual Meeting of the Association for Computational Linguistics (Volume 1: Long Papers)*, pages 23078–23097. Association for Computational Linguistics, 2025. doi: 10.18653/v1/2025.acl-long.1126. URL <https://aclanthology.org/2025.acl-long.1126/>.
- Manzil Zaheer, Guru Guruganesh, Kumar Avinava Dubey, Joshua Ainslie, Chris Alberti, Santiago Ontanon, Philip Pham, Anirudh Ravula, Qifan Wang, Li Yang, and Amr Ahmed. Big Bird: Transformers for longer sequences. In H. Larochelle, M. Ranzato, R. Hadsell, M.F. Balcan, and H. Lin, editors, *Advances in Neural Information Processing Systems*, volume 33, pages 17283–17297. Curran Associates, Inc., 2020.
- Jintao Zhang, Chendong Xiang, Haofeng Huang, Jia Wei, Haocheng Xi, Jun Zhu, and Jianfei Chen. SpargeAttention: Accurate and training-free sparse attention accelerating any model inference. In Aarti Singh, Maryam Fazel, Daniel Hsu, Simon Lacoste-Julien, Felix Berkenkamp, Tegan Maharaj, Kiri Wagstaff, and Jerry Zhu, editors, *Proceedings of the 42nd International Conference on Machine Learning*, volume 267 of *Proceedings of Machine Learning Research*, pages 76397–76413. PMLR, 2025. URL <https://proceedings.mlr.press/v267/zhang25ch.html>.
- Zhenyu Zhang, Ying Sheng, Tianyi Zhou, Tianlong Chen, Lianmin Zheng, Ruisi Cai, Zhao Song, Yuandong Tian, Christopher Ré, Clark Barrett, Zhangyang Wang, and Beidi Chen. H2O: Heavy-hitter oracle for efficient generative inference of large language models. In *Advances in Neural Information Processing Systems*, volume 36, 2023.

6 UPPER BOUNDS ANALYSIS FOR DUAL STAGE SPARSE ATTENTION DESIGN

The scaled-dot product attention can be written as follows,

$$\mathbf{A} = \mathbf{D}_s^{-1} \exp\left(\frac{\mathbf{Q}\mathbf{K}^\top}{\sqrt{C}}\right) \odot \mathbf{Z}_s, \quad \mathbf{O}_s = \mathbf{A}\mathbf{V}, \quad (28)$$

where \mathbf{Z}_s is a causal mask and $\mathbf{D}_s^{-1} \in \mathbb{R}^{N \times N}$ is a diagonal matrix of which each diagonal element is the inverse of the sum of the corresponding row of $\exp\left(\frac{\mathbf{Q}\mathbf{K}^\top}{\sqrt{C}}\right) \odot \mathbf{Z}_s$.

To characterize the difference between \mathbf{O} and \mathbf{O}_s , we need to first introduce Remark 1,

Remark 1. Let $i = 1, 2, \dots, N$ and $j = 1, 2, \dots, N$,

$$\begin{aligned} \mathbf{Z}_{\mathbf{M}(i,j)=1}(i,j) &= 1, \\ \mathbf{Z}_{\mathbf{M}(i,j)=-\infty}(i,j) &= 0, \end{aligned}$$

where \mathbf{M} is an importance mask matrix. Therefore, one has

$$\mathbf{A}_2 = \mathbf{D}^{-1} \exp\left(\frac{\mathbf{Q}\mathbf{K}^\top}{\sqrt{C}}\right) \odot \mathbf{Z}, \quad \mathbf{O} \leftarrow \mathbf{A}_2 \mathbf{V}. \quad (29)$$

where $\mathbf{D}^{-1} \in \mathbb{R}^{m \times m}$ is a diagonal matrix of which each diagonal element is the inverse of the sum of the corresponding row of $\exp\left(\frac{\mathbf{Q}\mathbf{K}^\top}{\sqrt{C}}\right) \odot \mathbf{Z}$.

Then we have,

$$\|\mathbf{A}_2 - \mathbf{A}\|_F \leq \underbrace{(\|\mathbf{D}^{-1}\mathbf{D}_s - \mathbf{I}\|_F \|\mathbf{Z}\|_F + \|\mathbf{Z} - \mathbf{Z}_s\|_F)}_{\alpha} \underbrace{\left\| \mathbf{D}_s^{-1} \exp\left(\frac{\mathbf{Q}\mathbf{K}^\top}{\sqrt{C}}\right) \right\|_F}_{\mathbf{A}},$$

which implies that

$$\|\mathbf{O} - \mathbf{O}_s\|_F = \|\mathbf{A}_2 \mathbf{V} - \mathbf{A} \mathbf{V}\|_F \leq \alpha \|\mathbf{A}\|_F \|\mathbf{V}\|_F. \quad (30)$$